

UDC 541.6:541.49:546.65

**DENSITY FUNCTIONAL THEORY INSIGHT INTO Eu(III) AND Am(III) COMPLEXES
WITH TWO 2,6-DICARBOXPYRIDINE DIAMIDE-TYPE LIGANDS**

Y. Yang¹, Y. Fang², Q. Liu², L. Yang¹, S. Hu¹, S. Hu², D. Wang³, H. Zhang², S. Luo¹

¹*Institute of Nuclear Physics and Chemistry, China Academy of Engineering Physics, Mianyang, Sichuan, P. R. China*

²*Key Laboratory of Radiopharmaceuticals of Ministry of Education, College of Chemistry, Beijing Normal University, Beijing, P.R. China*

³*College of Chemistry, Sichuan University, Chengdu, P. R. China*

Received May, 25, 2015

Revised — October, 21, 2015

Extraction complexes of Eu(III) and Am(III) with two 2,6-dicarboxypyridine diamide-type ligands L—A and L—B (Fig. 1) are studied by density functional theory (DFT). At both B3LYP/6-31G(d)/RECP and MP2/6-31G(d)/RECP levels of theory, the geometrical optimizations of the structures of the complexes can achieve the same accuracy and obtain the same geometrical configuration. At the B3LYP/6-311G(d,p)/RECP level of theory Eu³⁺ and Am³⁺ prefer to form [ML]³⁺ complexes under the solvation conditions, and the Am(III) complexes with L—A are more stable than the corresponding Eu(III) complexes. In the system with the ligand L—B, both [ML]³⁺ and [ML(NO₃)₃] species are very unstable.

DOI: 10.15372/JSC20170405

К e y w o r d s: density functional theory, second order Moller-Plesset perturbation theory, selective extraction, natural bond orbital analysis.

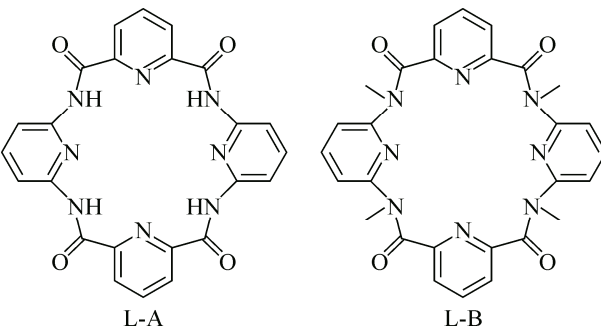
INTRODUCTION

To reduce the long-term radiological hazards of high-level nuclear waste (HLW), radionuclides with long half-lives need to be separated and converted into isotopes that are stable or short-lived via a strategy called partitioning and transmutation (P&T) [1, 2]. Extractive separation of the trivalent actinides Am(III) and Cm(III) from lanthanides (Ln(III)) is one of the most difficult steps in the P&T strategy because of similar chemical properties of An(III) and Ln(III). In the past two decades, many ligands have been designed in attempts to efficiently separate Am(III) from Ln(III). Alkyl-substituted amides have been proposed to be promising ligands for actinides extraction. These ligands not only effectively extract Am(III) [3—7] but also extract tetra- and hexavalent actinides. The amide derivatives of dipicolinic acid (DPA) exhibit good selectivity for Am(III) over Ln(III) because of the "soft" pyridine donor nitrogen in the structure. A number of studies have been conducted with hexavalent (e.g., U(VI)) and trivalent actinides which have demonstrated that DPA diamides can effectively extract these actinides into polar fluorinated diluents from highly acidic (2—6 M HNO₃) solutions [8—10].

Radiolytic stability is one of the critical characteristics of a candidate ligand for radioactive waste processing. It has been demonstrated that in solution dipicolinamides are easily radiolyzed to the corresponding amine and carboxylic acid, but branching of the alkyl group of dipicolinamides bound to the N atom reduces the radiolytic degradation [11]. Macroyclic compounds, such as crown ether,

Fig. 1. The structures of the L—A and L—B ligands

calixarene, and calix-crown-ether, are efficient extractants for ^{90}Sr and ^{137}Cs with high selectivity and have good radiolytic stability because of their cycle structures [12]. In this work, we designed new macrocyclic compounds based on 2,6-dipicolinamide (L—A and L—B as shown in Fig. 1) in attempt to improve the radiolytic stability of the ligands. However, experimental investigations are impeded since the actinides are in short supply and highly radioactive. In contrast, theoretical studies are alternative methods for studying coordination with new ligands. In the present study, quantum mechanical (QM) calculations are used to investigate the separation of Am(III) from Eu(III) in nitric acid solution. We shall systematically discuss the equilibrium geometries, electronic structures, and stabilities of the Eu(III) and Am(III) extraction complexes.



THEORETICAL

The 3D structures of these complexes were constructed, and a systematic search was performed with SYBYL-X 1.3 [13] to find the preferred conformations of the complexes. For the geometrical optimizations, the quasi-relativistic effective core potentials (RECP) and the corresponding valence basis sets were used for the Eu and Am atoms that included 28 and 60 electrons in the core, respectively, while the 6-31G(*d*) basis sets were adopted for the other atoms including C, H, O, and N. The geometrical optimizations were undertaken at both the B3LYP/6-31G(*d*)/RECP and MP2/6-31G(*d*)/RECP levels of theory. Next, we performed electronic calculations with the density functional theory (DFT) method for all of the species at the B3LYP/6-31G(*d*)/RECP theoretical level (RECP = = the quasi-relativistic effective core potential). At the B3LYP/6-311G(*d,p*)/RECP level, the gas-phase Gibbs binding energies (ΔG_g) were obtained, which included the zero-point and thermal corrections. We also calculated the solvation Gibbs binding energies (ΔG_{solv}) in water with a conductor-like polarizable continuum model (CPCM) [14, 15] with the default atomic radii based on the optimized structures in the gas phase. We used the Gaussian 09 vB.01 code [16] to perform all of the computations. The combination of continuum theory and quantum mechanics has been applied widely to the description of the reaction mechanisms. The CPCM, in which the interaction of the solute and the solvent are described via continuum model, is a relatively commonly used model among many models. The relative solvation binding energies include the electrostatic binding energies and the non-electrostatic binding energies and can be described as follows:

$$\Delta G_{\text{solv}} = \Delta G_g + \Delta \Delta G_{\text{solv}}, \quad (1)$$

where the "relative" Gibbs binding energies of solvation $\Delta \Delta G_{\text{solv}}$ include the electrostatic and non-electrostatic components as described by equation (2)

$$\Delta \Delta G_{\text{solv}} = \Delta G_{\text{el}} + \Delta G_{\text{non}} = \Delta G_{\text{el}} + \Delta G_{\text{cav}} + \Delta G_{\text{dis}} + \Delta G_{\text{rep}}. \quad (2)$$

The terms ΔG_{el} , ΔG_{non} , ΔG_{cav} , ΔG_{dis} , and ΔG_{rep} are the total electrostatic binding energies, the total non-electrostatic binding energies, the cavitation energy, the dispersion energy, and the repulsion energy, respectively.

RESULTS AND DISCUSSION

L—A type extraction complexes. Geometrical structures. The optimized geometrical structures of the extraction complexes with the L—A ligand are shown in Fig. 2. At both B3LYP/6-31G(*d*)/RECP and MP2/6-31G(*d*)/RECP levels of theory, the structure of free L—A is essentially planar, but in the $[\text{ML}]^{3+}$ species, the four aromatic rings are not in the same plane, but form a saddle-shaped structure. The four-coordinated complexes are formed via the metal atom coordinating with the four aromatic N atoms on the four aromatic rings. We can also see that the four aromatic rings are also

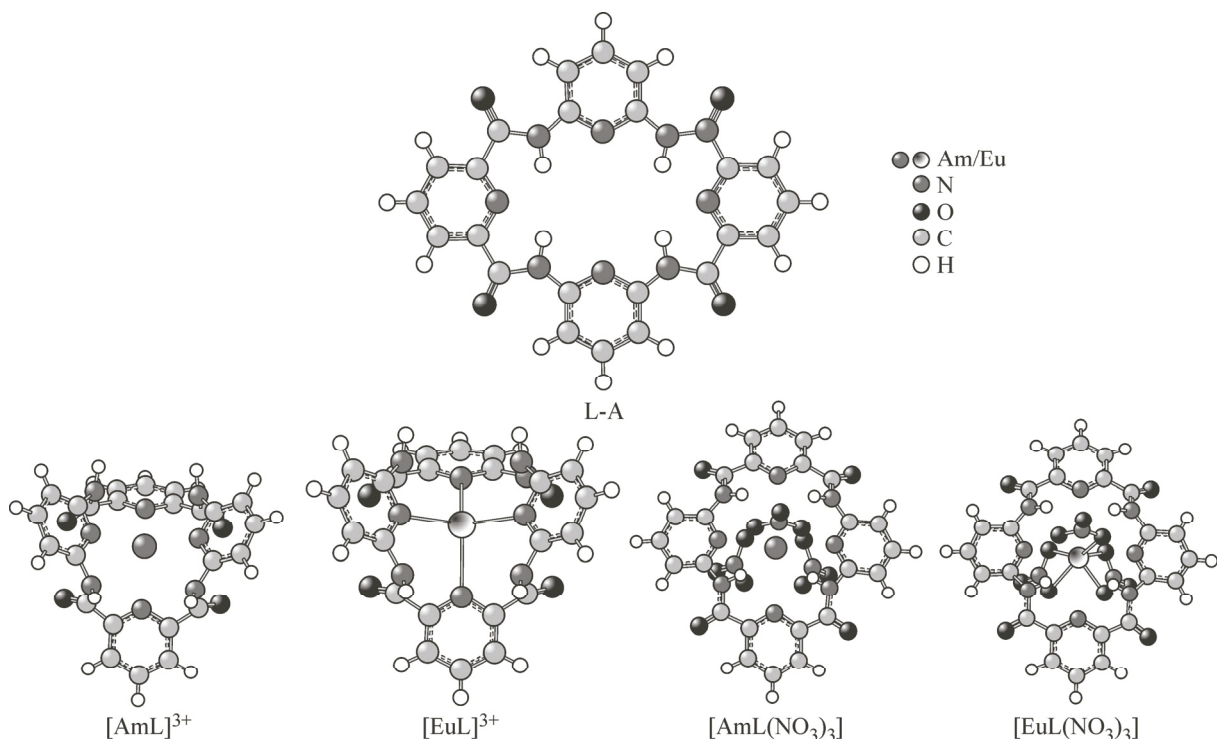


Fig. 2. Optimized structures of the Am(III) and Eu(III) complexes with the L—A ligand.

not in the same plane in the structures of the $[ML(NO_3)_3]$ species. The metal atom coordinates with the two aromatic N atoms of the four aromatic rings and the six O atoms on the nitrate ions to form the 8-coordinated complexes.

There is little difference between the bond lengths calculated at the B3LYP/6-31G(*d*)/RECP level and those calculated at the MP2/6-31G(*d*)/RECP level, as shown in Table 1. This suggests that in the

Table 1

Calculated M—N and M—O bond lengths (\AA) for the Eu^{3+} and Am^{3+} complexes with L—A ligands by the B3LYP and the MP2 methods^a

Species	M—N1 ^b	M—N2	M—N3	M—N4	M—O1
Species	M—O2	M—O3	M—O4	M—O5	M—O6
$[\text{Am}(\text{L—A})]^{3+}$	2.647/2.641	2.647/2.648	2.442/2.444	2.442/2.450	/
$[\text{Eu}(\text{L—A})]^{3+}$	2.611/2.608	2.611/2.612	2.419/2.420	2.419/2.423	/
$[\text{Am}(\text{L—A})(\text{NO}_3)_3]$	/	/	2.779/2.778	2.779/2.786	2.668/2.663
$[\text{Eu}(\text{L—A})(\text{NO}_3)_3]$	/	/	2.784/2.788	2.771/2.779	2.652/2.650
$[\text{Am}(\text{L—A})]^{3+}$	/	/	/	/	/
$[\text{Eu}(\text{L—A})]^{3+}$	/	/	/	/	/
$[\text{Am}(\text{L—A})(\text{NO}_3)_3]$	2.669/2.664	2.429/2.438	2.429/2.433	2.429/2.424	2.429/2.422
$[\text{Eu}(\text{L—A})(\text{NO}_3)_3]$	2.706/2.702	2.389/2.397	2.389/2.391	2.391/2.386	2.391/2.386

^a The N1, N2, N3, and N4 atoms are the four aromatic N atoms in the complexes. The O1, O2, O3, O4, O5, and O6 atoms are the six O atoms on the nitrate ions in the complexes.

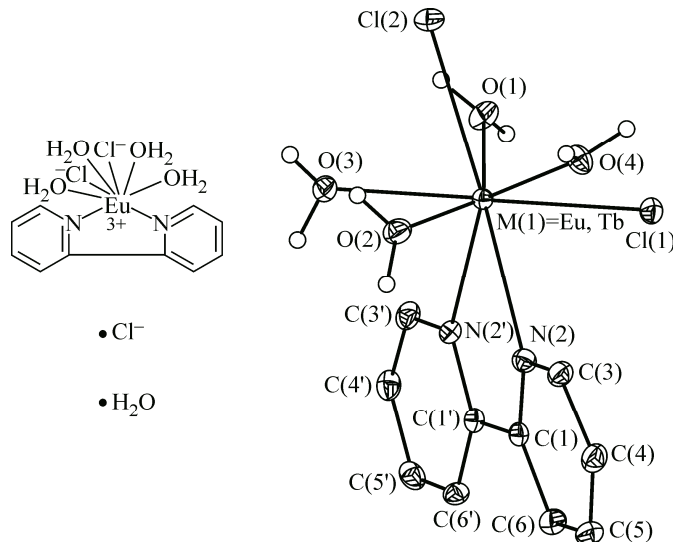
^b .../... refers to the results of the complexes calculated at the B3LYP/6-31G(*d*)/RECP and the MP2/6-31G(*d*)/RECP levels, respectively.

Fig. 3. The chemical structure and the ORTEP view of a complex Eu—A (structurally similar to our complexes) which was crystallographically characterized in a previous report

calculations of the molecular configuration, the B3LYP and MP2 methods achieve the same accuracy with the 6-31G(*d*) basis set. The bond lengths formed between the metal ions and the N atoms in the [ML(NO₃)₃] species are expectedly longer than those of the [ML]³⁺ species.

Because there are no crystallographic data available for these complexes we searched for a crystallographically characterized complex in a previous report that would be structurally similar to our complexes, such as [Eu(bipy)(H₂O)₄Cl₂]⁺ (Fig. 3). The geometrical optimizations were then undertaken at the B3LYP/6-31G(*d*)/RECP level based on the crystallographic data file of the complex. The optimization results are generally consistent with the crystallographic data, as shown in Table 2. These results also prove the reliability of the B3LYP (DFT) method for our complexes [17].

Energetics of the [ML]³⁺ and [ML(NO₃)₃] complexes. First, the gas phase Gibbs energies (ΔG_g) and the solvation Gibbs energies (ΔG_{solv}) of the Am(III) and Eu(III) the complexes with the L—A ligand were calculated, both when the spin multiplicity of the metal complexes was 1, and when it was 3. It can be seen from Table 3 that when the spin multiplicity of the metal complexes were 1, whether



Comparison of the bond lengths (Å) shown in crystallographic data to those calculated by the B3LYP method for the complex Eu—A^a

Bond	Bond length ^a	Bond	Bond length	Bond	Bond length	Bond	Bond length
M—Cl(1)	2.749/2.757	M—O(1)	2.406/2.401	M—O(3)	2.465/2.468	M—N(2)	2.566/2.546
M—Cl(2)	2.748/2.751	M—O(2)	2.419/2.439	M—O(4)	2.405/2.420	M—N(2')	2.575/2.573

^a .../... refers to the bond lengths (Å) shown in the crystallographic data and those calculated by the B3LYP method, respectively.

Table 3

Energetics of the [M(L—A)]³⁺ and [M(L—A)(NO₃)₃] complexes

Complexes	Spin Multiplicity	ΔG_g , a.u.	$\Delta \Delta G_{\text{solv}}$, kcal/mol	$\Delta \Delta G_{\text{solv}}$, a.u.	ΔG_{solv} , a.u.
[Am(L—A)] ³⁺	1	-2257.27	-312.54	-0.50	-2257.77
	3	-2257.20	-310.63	-0.50	-2257.70
[Eu(L—A)] ³⁺	1	-2372.16	-303.99	-0.48	-2372.64
	3	-2372.14	-281.93	-0.45	-2372.59
[Am(L—A)(NO ₃) ₃]	1	-3099.24	7.09	0.01	-3099.22
	3	-3099.15	7.95	0.01	-3099.14
[Eu(L—A)(NO ₃) ₃]	1	-3214.12	8.81	0.01	-3214.11
	3	-3214.05	9.60	0.02	-3214.04

Table 4

Theoretical complexation energies (kcal/mol) of the metal complexes with the L—A ligand by the B3LYP method

Reaction	ΔG_g	ΔG_{solv}
$[\text{Am}(\text{NO}_3)(\text{H}_2\text{O})_7]^{2+} + \text{L—A} \rightarrow [\text{Am}(\text{L—A})]^{3+} + \text{NO}_3^- + 7\text{H}_2\text{O}$	136.6	-110.0
$[\text{Eu}(\text{NO}_3)(\text{H}_2\text{O})_7]^{2+} + \text{L—A} \rightarrow [\text{Eu}(\text{L—A})]^{3+} + \text{NO}_3^- + 7\text{H}_2\text{O}$	136.9	-100.3
$[\text{Am}(\text{NO}_3)(\text{H}_2\text{O})_7]^{2+} + \text{L—A} + 2\text{NO}_3^- \rightarrow [\text{Am}(\text{L—A})(\text{NO}_3)_3] + 7\text{H}_2\text{O}$	-275.8	-25.4
$[\text{Eu}(\text{NO}_3)(\text{H}_2\text{O})_7]^{2+} + \text{L—A} + 2\text{NO}_3^- \rightarrow [\text{Eu}(\text{L—A})(\text{NO}_3)_3] + 7\text{H}_2\text{O}$	-275.5	-22.6

in vacuum or under solvation, the metal complexes with the ligand L—A are in the ground state. Therefore we discuss only the case with spin multiplicity 1.

It can be observed from Table 4 that the majority of the gas phase Gibbs binding energies (ΔG_g) and the solvation Gibbs binding energies (ΔG_{solv}) are negative, with the exception that ΔG_g of the $[\text{ML}]^{3+}$ species are positive. For the $[\text{ML}]^{3+}$ species, ΔG_{solv} are negative while ΔG_g are positive, indicating that the solvation is beneficial to the coordination to form the $[\text{ML}]^{3+}$ species. In contrast, solvation is unfavorable to the formation of the $[\text{ML}(\text{NO}_3)_3]$ species, since ΔG_{solv} are much lower than ΔG_g for the $[\text{ML}(\text{NO}_3)_3]$ species. Additionally, ΔG_{solv} of the $[\text{ML}]^{3+}$ species were found to be much higher than those of the corresponding neutral $[\text{ML}(\text{NO}_3)_3]$ complexes. Therefore, $[\text{ML}]^{3+}$ are the preferred complexes for Eu^{3+} and Am^{3+} to form with L—A under the solvation condition.

Moreover, relatively higher ΔG_{solv} of the $[\text{AmL}]^{3+}$ and the $[\text{AmL}(\text{NO}_3)_3]$ species, compared to ΔG_{solv} of the corresponding Eu(III) complexes, imply that the Am(III) complexes are more stable than the corresponding Eu(III) complexes.

L—B type extraction complexes. Geometrical optimizations and structural aspects. Fig. 4 shows the optimized geometrical structures of the extraction complexes with the L—B ligand. Both free L—B ligand structure and structures of the complexes are not planar, at both B3LYP/6-31G(d)/RECP and MP2/6-31G(d)/RECP levels of theory. The structures of the $[\text{ML}]^{3+}$ species show that the metal atom coordinates with the three aromatic N atoms from three of the four aromatic rings. From the structures of the $[\text{ML}(\text{NO}_3)_3]$ species we can see that the four aromatic rings are not in the same plane. The metal atom coordinates with the aromatic N atom from only one of the four aromatic rings, and with the six O atoms on the nitrate ions.

As shown in Table 5, the B3LYP method is as accurate as the MP2 method when using the 6-31G(d) basis set. Moreover, the coordination interactions in the $[\text{M}(\text{L—B})]^{3+}$ and $[\text{M}(\text{L—B})(\text{NO}_3)_3]$ species might be weaker than those in the corresponding $[\text{M}(\text{L—A})]^{3+}$ and $[\text{M}(\text{L—A})(\text{NO}_3)_3]$ species, because there are fewer coordination bonds between the metal atoms and L—B ligand than with the L—A ligand. The complexes formed between the metal atom and the L—B ligand might be therefore unstable.

Energetics of the $[\text{ML}]^{3+}$ and $[\text{ML}(\text{NO}_3)_3]$ complexes. The gas phase Gibbs energies (ΔG_g) and the solvation Gibbs energies (ΔG_{solv}) with the L—B ligand were calculated (Table 6). We discuss the metal complexes with the L—B ligand when their spin multiplicity was 1.

From Table 7 we can conclude that the majority of the gas phase Gibbs binding energies (ΔG_g) and the solvation Gibbs binding energies (ΔG_{solv}) are positive, with the exception that ΔG_g of the $[\text{ML}(\text{NO}_3)_3]$ species are negative, which indicates that most of the coordination interactions are very weak and not inclined to form complexes, with the exception of the formation of $[\text{ML}(\text{NO}_3)_3]$ species in the gas phase. Therefore, regardless of whether the $[\text{ML}]^{3+}$ species or the $[\text{ML}(\text{NO}_3)_3]$ species are involved, the Am(III) and Eu(III) complexes that form between the metal atoms and the L—B ligand cannot be stable to exist in solution, and the L—B ligand is not an eligible extractant.

Natural bond orbital analysis of $[\text{ML}]^{3+}$ and the $[\text{ML}(\text{NO}_3)_3]$ complexes with the L—A and L—B ligands. As shown in Table 8, the M—N and M—O bonds are primarily ionic and regulated by the electrostatic interactions because, for all of the M—N and the M—O bonds in these extraction

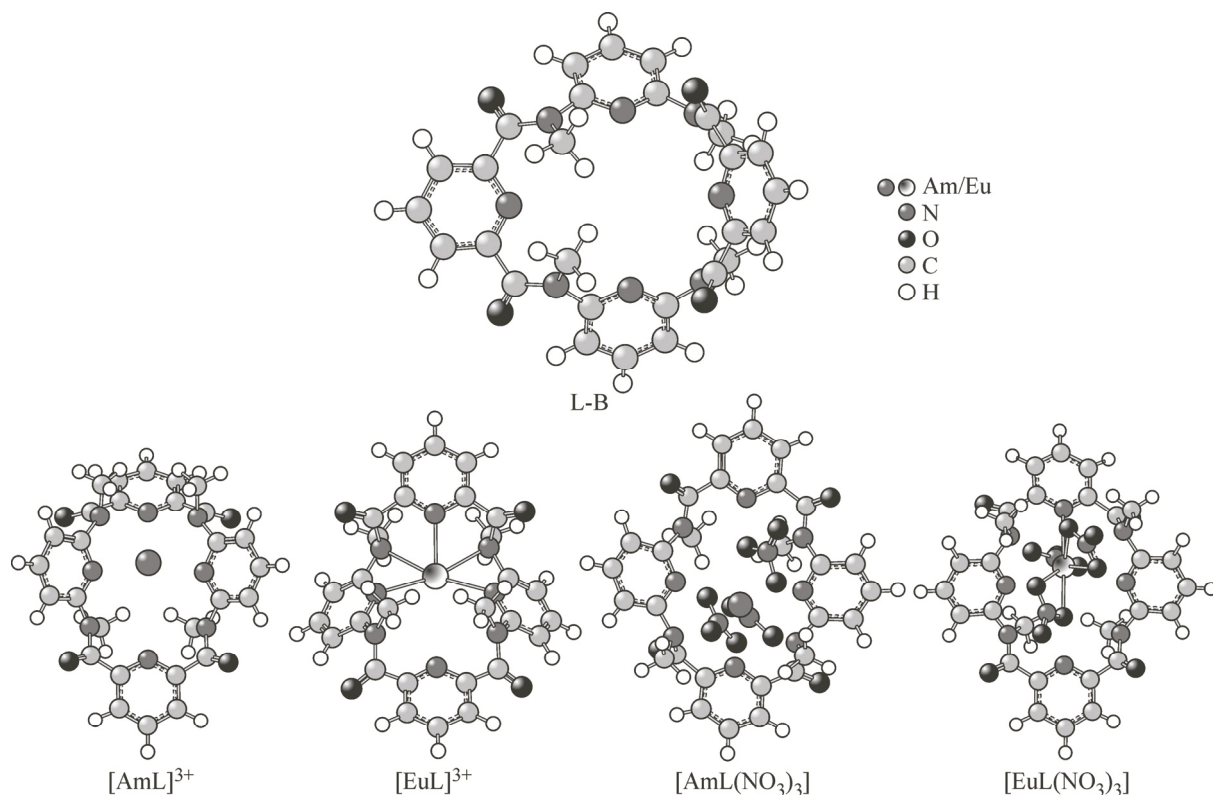


Fig. 4. Optimized structures of the Am(III) and Eu(III) complexes with the L—B ligand and the L—B ligand.

complexes, the Wiberg bond indices (WBIs) are between 0.203 and 0.332. We can also infer that the metal—ligand bonds in the $[ML(NO_3)_3]$ species are more ionic, based on the smaller M—O and M—N WBIs relative to those of the $[ML]^{3+}$ species. Additionally, there appear a higher degree of co

Table 5

Calculated M—N and M—O bond lengths (\AA) for the Eu^{3+} and Am^{3+} complexes with L—B ligand by the B3LYP and the MP2 methods^a

Species	M—N1 ^b	M—N2	M—N3	M—N4	M—O1
$[\text{Am}(\text{L—B})]^{3+}$	2.453/2.449	2.448/2.448	2.448/2.457	/	/
$[\text{Eu}(\text{L—B})]^{3+}$	2.410/2.408	2.452/2.448	2.452/2.449	/	/
$[\text{Am}(\text{L—B})(\text{NO}_3)_3]$	2.690/2.694	/	/	/	3.597/3.600
$[\text{Eu}(\text{L—B})(\text{NO}_3)_3]$	2.642/2.649	/	/	/	2.852/2.856
Species	M—O2	M—O3	M—O4	M—O5	M—O6
$[\text{Am}(\text{L—B})]^{3+}$	/	/	/	/	/
$[\text{Eu}(\text{L—B})]^{3+}$	/	/	/	/	/
$[\text{Am}(\text{L—B})(\text{NO}_3)_3]$	2.367/2.362	2.504/2.524	2.418/2.415	2.468/2.483	2.483/2.463
$[\text{Eu}(\text{L—B})(\text{NO}_3)_3]$	2.429/2.424	2.377/2.320	2.475/2.476	2.496/2.496	2.453/2.454

^a The N1, N2, N3, and N4 atoms are the four aromatic N atoms in the complexes. The O1, O2, O3, O4, O5, and O6 atoms are the six O atoms on the nitrate ions in the complexes.

^b .../... refers to the results of the complexes calculated at the B3LYP/6-31G(d)/RECP and MP2/6-31G(d)/RECP levels, respectively.

Table 6

Energetics of the $[M(L-B)]^{3+}$ and $[M(L-B)(NO_3)_3]$ complexes

Complex	Spin multiplicity	ΔG_g , a.u.	$\Delta\Delta G_{solv}$, kcal/mol	$\Delta\Delta G_{solv}$, a.u.	ΔG_{solv} , a.u.
$[Am(L-A)]^{3+}$	1	-2414.38	-308.10	-0.49	-2414.88
	3	-2414.29	-299.70	-0.48	-2414.77
$[Eu(L-A)]^{3+}$	1	-2529.29	-305.14	-0.49	-2529.78
	3	-2529.27	-293.57	-0.47	-2529.73
$[Am(L-A)(NO_3)_3]$	1	-3256.33	12.64	0.02	-3256.31
	3	-3256.24	13.50	0.02	-3256.22
$[Eu(L-A)(NO_3)_3]$	1	-3371.20	12.40	0.02	-3371.18
	3	-3371.13	13.60	0.02	-3371.11

Table 7

Theoretical complexation energies (kcal/mol) of the metal complexes with ligand L—B by the B3LYP method^a

Reactions	ΔG_g	ΔG_{solv}
$[Am(NO_3)(H_2O)_7]^{2+} + L-B \rightarrow [AmL(L-B)]^{3+} + NO_3^- + 7H_2O$	385.4	139.4
$[Eu(NO_3)(H_2O)_7]^{2+} + L-B \rightarrow [Eu(L-B)]^{3+} + NO_3^- + 7H_2O$	373.7	130.6
$[Am(NO_3)(H_2O)_7]^{2+} + L-B + 2NO_3^- \rightarrow [Am(L-B)(NO_3)_3] + 7H_2O$	-16.0	236.1
$[Eu(NO_3)(H_2O)_7]^{2+} + L-B + 2NO_3^- \rightarrow [Eu(L-B)(NO_3)_3] + 7H_2O$	-6.2	246.5

Table 8

Theoretical wiberg bond indices (WBIs) of the relative coordination bonds for the Eu(III) and Am(III) complexes with L—A and L—B in the NAO basis by the B3LYP method^a

Species	M—N1	M—N2	M—N3	M—N4	M—O1	M—O2	M—O3	M—O4	M—O5	M—O6
$[Am(L-A)]^{3+}$	0.283	0.283	0.332	0.332	/	/	/	/	/	/
$[Eu(L-A)]^{3+}$	0.257	0.257	0.318	0.318	/	/	/	/	/	/
$[Am(L-A)(NO_3)_3]$	/	/	0.212	0.214	0.294	0.291	0.368	0.368	0.368	0.368
$[Eu(L-A)(NO_3)_3]$	/	/	0.203	0.203	0.292	0.275	0.367	0.367	0.366	0.366
$[Am(L-B)]^{3+}$	/	0.302	0.309	0.309	/	/	/	/	/	/
$[Eu(L-B)]^{3+}$	/	0.293	0.295	0.295	/	/	/	/	/	/
$[Am(L-B)(NO_3)_3]$	/	0.248	/	/	0.212	0.422	0.394	0.348	0.326	0.345
$[Eu(L-B)(NO_3)_3]$	/	0.235	/	/	0.064	0.379	0.381	0.334	0.320	0.332

^a The N1, N2, N3, and N4 atoms are the four aromatic N atoms in the complexes. The O1, O2, O3, O4, O5, and O6 atoms are the six O atoms on the nitrate ions in the complexes.

valence in the M—O bonds as compared to the M—N bonds in the $[ML(NO_3)_3]$ species. Notably, the result that the M—O and the M—N WBIs of the Am(III) extraction complexes are slightly larger in most cases than those of the corresponding Eu(III) extraction complexes, seems to comply with the more covalent character of the actinide bonding compared to the lanthanide bonding [18, 19].

Table 9 shows the gross orbital populations of the *s*, *p*, *d*, and *f* valence shells on the Am and Eu atoms and Mulliken atomic charges of the atoms that participate in the coordination. In most cases, the Eu³⁺ species have lower *s*, *p* and *f* orbital populations than the Am³⁺ species do, while the Am³⁺ species have lower *d* orbital populations. It can also be concluded that important electronic charge transfer

Table 9

B3LYP Mulliken orbital populations (*s, p, d, and f*) and natural charges on the metal and N or O atoms for the Eu(III) and Am(III) complexes with L—A and L—B^a for the Eu(III) and Am(III) complexes with L—A and L—B in the NAO basis by the B3LYP method^a

Species	M—N1	M—N2	M—N3	M—N4	M—O1	M—O2	M—O3	M—O4	M—O5	M—O6
[Am(L—A)] ³⁺	0.283	0.283	0.332	0.332	/	/	/	/	/	/
[Eu(L—A)] ³⁺	0.257	0.257	0.318	0.318	/	/	/	/	/	/
[Am(L—A)(NO ₃) ₃]	/	/	0.212	0.214	0.294	0.291	0.368	0.368	0.368	0.368
[Eu(L—A)(NO ₃) ₃]	/	/	0.203	0.203	0.292	0.275	0.367	0.367	0.366	0.366
[Am(L—B)] ³⁺	/	0.302	0.309	0.309	/	/	/	/	/	/
[Eu(L—B)] ³⁺	/	0.293	0.295	0.295	/	/	/	/	/	/
[Am(L—B)(NO ₃) ₃]	/	0.248	/	/	0.212	0.422	0.394	0.348	0.326	0.345
[Eu(L—B)(NO ₃) ₃]	/	0.235	/	/	0.064	0.379	0.381	0.334	0.320	0.332

^a The N1, N2, N3, and N4 atoms are the four aromatic N atoms in the complexes. The O1, O2, O3, O4, O5, and O6 atoms are the six O atoms on the nitrate ions in the complexes.

from the ligands to the metal atoms occurs, because the natural charges on the Eu and Am atoms range from 1.160 to 1.535.

CONCLUSIONS

The geometrical structures, electronic structures, and the stabilities of the Eu(III) and Am(III) extraction complexes with two 2,6-dicarboxypyridine diamide-type ligands were examined with the B3LYP method and primarily using density functional theory (DFT). The optimizations of the structures achieve the same accuracy and obtain the same geometrical configuration at both the B3LYP/6-31G(*d*)/RECP and MP2/6-31G(*d*)/RECP levels of theory. At the B3LYP/6-311G(*d,p*)/RECP level and in the complex system with ligand L—A, Eu³⁺ and Am³⁺ prefer to form [ML]³⁺ complexes under the solvation condition, and the Am(III) complexes are more stable than the corresponding Eu(III) complexes. In the complex system with the L—B ligand, the complexes, regardless of whether the [ML]³⁺ or the [ML(NO₃)₃] species is involved, are unstable. Therefore, the L—B ligand is not an eligible extractant. Further in-depth investigations should be undertaken.

The authors declare no potential competing financial interests.

This work was supported by the National Major Scientific and Technological Special Project for "Significant New Drugs Development" (Grant Nos. 2014ZX09507007-001 and 2014ZX09507007-003); the National Science and Technology Support Program (Grant No. 2014BAA03B03); and the National Natural Science Foundation of China (Grant Nos. 21371026).

The authors declare that the research involved no human participants and no animal.

REFERENCES

1. Nash K.L., Choppin G.R. // Sep. Sci. Technol. – 1997. – **32**, N 1. – P. 255 – 274.
2. Sood D.D., Patil S.K.R. // J. Radioanal. Nucl. Chem. – 1996. – **203**, N 2. – P. 547 – 573.
3. Alyapyshev M.Yu., Babain V.A., Tkachenko L.I., Eliseev I.I., Didenko A.V., Petrov M.L.R. // Solvent Extr. Ion Exch. – 2011. – **29**, N 4. – P. 619 – 636.
4. Cuillerdier C., Musikas C., Hoel P., Nigond L., Vitart X. // Sep. Sci. Technol. – 1991. – **26**, N 9. – P. 1229 – 1244.
5. Modolo G., Vijgen H., Serrano-Purroy D., Christiansen B., Malmbeck R., Sorel C., Baron P. // Sep. Sci. Technol. – 2007. – **42**, N3. – P. 439 – 452.
6. Sasaki Y., Tachimori S. // Solv. Extr. Ion Exch. – 2002. – **20**, N 1. – P. 21 – 34.
7. Zhu Z.-X., Sasaki Y., Suzuki H., Suzuki S., Kimura T. // Anal. Chim. Acta. – 2004. – **527**, N 2. – P. 163 – 168.

8. Lapka J.L., Paulenova A., Alyapyshev M.Y., Babain V.A., Herbst R.S., Law J.D. // Radiochim. Acta. – 2009. – **97**, N 6. – P. 291 – 296.
9. Paulenova A., Alyapyshev M.Y., Babain V.A., Herbst R.S., Law J.D. // Sep. Sci. Technol. – 2008. – **43**, N 9. – P. 2606 – 2618.
10. Babain V.A., Alyapyshev M.Y., Kiseleva R.N. // Radiochim. Acta. – 2007. – **95**, N 4. – P. 217 – 223.
11. Mowafy E.A. // Radiochim. Acta. – 2007. – **95**, N 9. – P. 539 – 545.
12. Xu C., Wang J., Chen J. // Solvent Extr. Ion Exc. – 2012. – **30**, N 6. – P. 623 – 650.
13. Sybyl, version X 1.3. – Tripos Associates: St. Louis, MO, 2011.
14. Tomasi J., Persico M. // Chem. Rev. – 1994. – **94**, N 7. – P. 2027 – 2094.
15. Chipman D.M. // J. Phys. Chem. A. – 2002. – **106**, N 32. – P. 7413 – 7422.
16. Frisch M.J., Trucks G.W., Schlegel H.B., Scuseria G.E., Robb M.A., Cheeseman J.R., Scalmani G., Barone V., Mennucci B., Petersson G.A., Nakatsuji H., Caricato M., Li X., Hratchian H.P., Izmaylov A.F., Bloino J., Zheng G., Sonnenberg J.L., Hada M., Ehara M., Toyota K., Fukuda R., Hasegawa J., Ishida M., Nakajima T., Honda Y., Kitao O., Nakai H., Vreven T., Montgomery J.A. Jr., Peralta J.E., Ogliaro F., Bearpark M., Heyd J.J., Brothers E., Kudin K.N., Staroverov V.N., Kobayashi R., Normand J., Raghavachari K., Rendell A., Burant J.C., Iyengar S.S., Tomasi J., Cossi M., Rega N., Millam J.M., Klene M., Knox J.E., Cross J.B., Bakken V., Adamo C., Jaramillo J., Gomperts R.E., Stratmann O., Yazev A.J., Austin R., Cammi C., Pomelli J.W., Ochterski R., Martin R.L., Morokuma K., Zakrzewski V.G., Voth G.A., Salvador P., Dannenberg J.J., Dapprich S., Daniels A.D., Farkas O., Foresman J.B., Ortiz J.V., Ciosowski J., Fox D.J. Gaussian 09, revision B.01. – Gaussian, Inc.: Wallingford, CT., 2010.
17. Puntus L.N., Lyssenko K., Pekareva I., Bunzli J. // J. Phys. Chem. B. – 2009. – **113**, N 27. – P. 9265 – 9277.
18. Reed A.E., Curtiss L.A., Weinhold F. // Chem. Rev. – 1988. – **88**, N 6. – P. 899 – 926.
19. Hill C. In: Ion Exchange, Solvent Extraction, A Series of Advances / Eds. B.A. Moyer. – Boca Raton: CRC Press, 2009. – P. 119 – 193.